



Integration of Low-Cost GNSS and Multispectral Camera to Increase Oil Palm Position Accuracy and Health Monitoring

M. N. Cahyadi ^{1*}, M. A. Syariz ¹, F. Taufany ², Lisnawita ³, S. S. Wismaroh ⁴,
D. Kusumawardani ⁵, T. B. Saputro ⁶, F. Haq ¹, M. C. Laksana ¹, L. A. Triawan ¹

¹ Department of Geomatics Engineering, Institut Teknologi Sepuluh Nopember, Surabaya 60111, Indonesia.

² Department of Chemical Engineering, Institut Teknologi Sepuluh Nopember, Surabaya 60111, Indonesia.

³ Program Study of Agrotechnology, Faculty of Agriculture, Universitas Sumatera Utara, 20155 Medan, Indonesia.

⁴ Department of Agrotechnology, Universitas Pembangunan Masyarakat Indonesia, Medan, Indonesia.

⁵ Department Economics, Faculty Economics and Business, Universitas Airlangga, Surabaya, Indonesia.

⁶ Department of Biology, Faculty of Science and Data Analytics, Institut Teknologi Sepuluh Nopember, Surabaya, Indonesia.

Received 25 November 2024; Revised 15 February 2025; Accepted 22 February 2025; Published 01 March 2025

Abstract

The Global Navigation Satellite System facilitates efficient agricultural initiatives, resolving land ownership and precise plantation monitoring issues. The oil palm sector is deeply integrated into various economies due to the world's use in food supplies, cosmetics, and oil biodiesel production. However, local farmers have trouble managing the plantation's condition and land ownership due to the underdeveloped modern technology at their disposal. The Normalized Difference Vegetation Index was employed in order to assess the NDVI camera oil palm tree growth, utilizing a MAPIR Survey3 RGN Multispectral Camera integrated with red, green, and near IR sensors. Images were taken directly on the surface level to enable focused analysis on the palm trees. This included the use of an MPAR calibration ground target placed beside the leaves for data accuracy and an operator that held the camera to the trees. Utilizing this strategy allowed for a more intricate and detailed analysis of each oil palm tree, and due to the coordination of the trees, aerial images were produced to create a detailed image. Low-cost GNSS instruments alongside RTK technology were employed in determining the coordinate position of the oil palm trees. Considerable relationships were found between NDVI and content in chlorophyll: NDVI-G and Chl *a* ($r = 0.679$), NDVI-B and Chl *a* ($r = 0.618$), and NDVI-B and Chl *b* ($r = 0.657$). The positional errors obtained varied within -0.105 to 0.166 meters for low-cost GNSS and -0.159 to 0.083 meters for geodetic GNSS, the latter recording the least MAE of 0.053 . This research work found a cheap and accurate oil palm growth monitoring system using multispectral sensors. This method overcomes the technological gap of local farmers and provides an alternative strategy for the management of plantations.

Keywords: Oil Palm; NDVI; Multispectral Camera; GNSS; Monitoring.

1. Introduction

Technological advancement is increasingly becoming a major focus in various industries, including oil palm, to efficiently monitor plant health and productivity. Monitoring plant development, mapping plantation areas, and identifying environmental changes play a crucial role in maintaining health and increasing productivity. However, one

* Corresponding author: cahyadi@geodesy.its.ac.id

<http://dx.doi.org/10.28991/CEJ-2025-011-03-010>



© 2025 by the authors. Licensee C.E.J, Tehran, Iran. This article is an open access article distributed under the terms and conditions of the Creative Commons Attribution (CC-BY) license (<http://creativecommons.org/licenses/by/4.0/>).

of the major challenges faced by local farmers is the limited access to technology for monitoring plant conditions and the high cost. This study focuses on developing a low-cost multispectral camera and a Real-Time Kinematic (RTK) observation method to improve positioning accuracy and overall oil palm health monitoring by the chlorophyll.

Several studies have been conducted using satellite imagery, including [1-3], which focused on monitoring the health of pine plants in the New Zealand region. These studies showed that by using NDVI spectral index modeling, an accuracy value of above 70% was obtained for changes in tree canopy color. NDVI measurements were carried out using RapidEye satellite imagery with a spatial resolution of 5 m. Multispectral imagery from Unmanned Aerial Vehicles (UAVs) was also used in the study by Dash et al. [1]. The UAV technology used was the MicaSense RedEdge 3 camera with a flight height during data acquisition of around 90 meters, which produced a Ground Sample Distance (GSD) of 6 cm. This study focused on tree areas in the forest. Hence, it was not able to assess the health of each tree individually [1]. UAV methodology can monitor each tree individually but requires low flight altitudes, increasing the risk of flight accidents [4, 5].

Considering that positioning is generally carried out separately from plant health monitoring, the coordinates obtained are not accompanied by information on oil palm health. In contrast, plant health is generally analyzed using NDVI values presented in the form of areas [6]. The use of NDVI refers to data transformation that allows the identification of oil palm plant health conditions by measuring vegetation cover in the canopy. This information does not provide details about the specific position of the plant, underscoring the need for integration with positional data, so the use of navigation technology is needed to improve the result. Therefore, a technology is needed to connect aspects of plant health, position, and oil palm GIS, which would be useful for detecting the health condition of each tree individually. This study aimed to conduct an analysis of oil palm plant health in smallholder oil palm plantations in Malang Regency and integrate this information with position data for accurate monitoring. The method is expected to provide more comprehensive and appropriate information for detecting the health condition of each oil palm tree individually and provide better information on position on plant area.

In a different context, Septiarini et al. [7] performed an analysis of palm oil leaf diseases containing image processing, involving the pixel counting function and color feature extraction. In this context, Otsu thresholding was employed in the Lab color space to identify areas of the leaf that are diseased, and the k-NN model was used to classify the leaves of the tree as healthy or non-healthy. It can be seen from the findings that diseases were successfully traced to the leaf level, but there was a failure to capture the geo-spatial nature of the data to geo-reference the diseased trees.

Low-cost NDVI technology has been developed by previous studies as an alternative solution to save operational costs for crop monitoring. Mazeh et al. [8] developed a low-cost multispectral NDVI sensor to detect weeds and estimate grape health, producing accurate NDVI values with an R^2 value of 0.87 but still found several different biases for each waveband. Low-cost NDVI developed by Stamford et al. [9] for analyzing plant health used a dual-camera system sensor priced at 380 USD connected to a Raspberry Pi, producing low-cost images, commonly referred to as NDVI. However, the study was limited to testing small plants such as *Phaseolus vulgaris* (French Bean). The method used Near-Infrared (NIR) and red wavebands from the camera sensor. NDVI_{pi} observations were validated with a spectrometer, and a statistical analysis yielded R^2 values ranging from 0.54 to 0.80. Additionally, the low-cost tool was compared to the Micasense RedEdge system, a commercial NDVI camera, which resulted in an R^2 of 0.70 to 0.90. The NDVI_{pi} camera sensor demonstrated good leaf measurement performance compared to standard spectrometric NDVI and commercial cameras [9].

Marzukhi et al. [10] highlighted that remote sensing technologies can be advanced to assess nutrient extent in oil palm, reinforcing the significance of multi-spectral images in health assessment. Tugi et al. [11] noted the use of UAVs for oil palm monitoring in smallholder plantations. However, the authors noted several drawbacks; high operational costs and technical expertise requirements for UAVs limit their adoption. More recent developments, such as affordable NDVI sensors like the NDVI_{pi} system, offer hope but are often limited to certain environments and small-scale settings.

The results of the NDVI transformation can define plant health conditions in a broad context. The NDVI value refers to the vegetation cover of oil palm, which is presented in the form of areas. Wang et al. [12] visualized health conditions based on the correlation between the NDVI value and validation of actual data using the spectrometer method with an R-value of 0.67. A common limitation across these approaches is the lack of integration between health data and precise spatial positioning. For instance, while NDVI data can effectively measure vegetation cover and health [6, 12], it is often presented as aggregated area-level information rather than tree-specific data. This limitation hinders targeted management strategies that require both positional accuracy and individual health analysis.

The advancement of monitoring technology has become a major focus in various industries, including agriculture. Technology continues to develop rapidly, providing better capabilities for monitoring plant health and productivity efficiently [13]. In the context of oil palm cultivation, monitoring technology should provide innovative solutions to track plant development, map plantation areas, and identify environmental changes that can affect plant health. The application of monitoring technology is key to increasing productivity and sustainability [14]. Plant health management

in the oil palm industry plays an important role in ensuring optimal growth and production. Various problems faced in cultivation include limited water for growth due to geological or weather factors. In addition, sanitation problems are also a serious concern because poor conditions can trigger the spread of disease and inhibit overall growth [15].

To address these gaps, this study combines low-cost GNSS technology with multispectral imaging to provide a comprehensive solution for monitoring oil palm health and spatial positioning. By leveraging a multispectral camera to calculate vegetation indices such as NDVI and integrating GNSS RTK for positional accuracy, the proposed approach offers a dual benefit. It enables precise mapping of individual tree health and position, thus supporting better decision-making in plantation management. The integration of these technologies is expected to enhance monitoring efficiency, reduce operational costs, and empower smallholder farmers with actionable insights for sustainable and efficient plantation practices [16, 17].

Positional databases are essential in the oil palm industry for managing the health of each plant. By monitoring the position and condition of each tree accurately, plantation managers can identify the trees that need special attention for watering, fertilization, or pesticide treatment. Information about plant positions also helps optimize the use of resources such as water, fertilizers, and pesticides, leading to reduced environmental impacts and increased production efficiency [18]. The positional database also enables managers to monitor changes in tree growth patterns and health over time. This helps in making better decisions for long-term planning and risk management strategies. Geographic information technology (GIS) and remote sensors allow for the collection of positional data more quickly and accurately. The NDVI analysis will help to ensure the condition of oil palm trees. This empowers plantation managers to develop more effective solutions to maintain the health of oil palm and ensure the sustainability of the industry [19]. Smallholder or plasma farmers require the use of technology to accurately assess the condition of oil palm plants. Accessible tools such as multispectral cameras can be a practical alternative to photographing objects and analyzing conditions visually. Therefore, this study aimed to perform health checks on plants using multispectral cameras and to track the location of oil palm trees using low-cost GNSS. Based on the previous research that NDVI can indicate the health condition of the tree coverage, not only the health condition that can be known by the research but also the information of such locations of the oil palm trees. The data collected from the cameras and GPS were combined to provide smallholder farmers with easily understandable information about the condition of oil palm trees. This research also added information on the position of the palm tree area that has such case conditions. The health of oil palm plants can be influenced by various factors, including soil nutrients and the presence of other crops [11, 15].

2. Research Methodology

In this study, the methodology involved several stages that utilized specific tools and technologies. Detailed specifications of these tools are presented in the following subsections.

2.1. Tool Specifications

To acquire accurate and relevant data, several tools with specific specifications were employed in this research. Each tool has a distinct role and characteristics that support data collection.

2.1.1. Multispectral Camera MAPIR Survey3 RGN

This study used images from the multispectral camera MAPIR Survey3 RGN, captured on 30 September 2023. The MAPIR Survey3 Cameras carry a triple band, namely, Red, Green, and NIR (Near-Infrared). The wavelengths for these bands are 550 nm, 660 nm, and 850 nm, respectively. MAPIR Survey3 Cameras, commonly referred to as Survey3, feature a no-fisheye lens with very low distortion, providing excellent results for aerial surveys [16]. The detailed images and specifications are shown in Table 1.

Table 1. Specifications of Multispectral Camera MAPIR Survey3 RGN

Image Resolution	12 MegaPixel (4000 × 3000 px), dan 8 MegaPixel
Image Format	RAW + JPG, (RAW is 12-bit, and JPG is 8bit)
Weight	50g (Without battery) 76g (With Battery)
Dimension	59 × 41.5 × 36 mm
ISO	50/ 100 / 200 / 400, Auto
Shutter Speed	1/2000, 1/1000, 1/500, 1/250, 1/125, 1/90, 1/60, 1/30, 1/15, 1/8, 1, 2, 3, 5, 10, 15, 20, 30, 60, Auto
Sensor	Red= 660 nm; Green = 550 nm; NIR= 850 nm

2.1.2. GNSS Geodetic – SinoGNSS T300

The SinoGNSS T300 is a geodetic-quality GNSS receiver. It supports navigation signals from multiple satellite systems, including GNSS (Global Navigation Satellite System), GPS (Global Positioning System), GLONASS, BeiDou, and Galileo, providing high-precision positioning. The available modes of the SinoGNSS T300 include Static, RTK, and RTK N-TRIP, with accuracy reaching centimeter-level fractions. The specifications of the SinoGNSS T300 are as follows.

Table 2. Specifications SinoGNSS T300

Satellite Signals	GPS L1 C/A, L1C, L2P, L5
	BeiDou B1, B2, B3
	GLONASS L1, L2
	Galileo Reserved
SBAS WAAS, EGNOS, MSAS, GAGAN	
Performance Specification	Cold starts <50s
	Warm start <30s
	Hot start <15s
	Initialization time 10s
	Signal re-acquisition <2s
Initialization reliability Typically>99.9	
Positioning Specification	Post Processing Static
	Horizontal: 2.5mm+0.5 ppm RMS
	Vertical: 5 mm+0.5 ppm RMS
	Real-Time Kinematic
	Horizontal: 8 mm+1 ppm RMS
	Vertical: 15 mm+ 1 ppm RMS
	E-RTK (<100 km)
Horizontal: 0.2 mm+1 ppm RMS	
Vertical: 0.4 mm+ 1 ppm RMS	

2.2. Data Collection

The oil palm plantation studied was owned by local farmers in Selorejo, Blitar Regency, East Java, as shown in Figure 1. The location featured sloping terrain; hence, there was a wet area on the west side and a dry area on the east side. This condition arose because the water flow, directed by the farmer, originates from a source on the west side of the study area. The irrigation method used by farmers consisted of water pipes directed under the oil palm trees in the form of irrigation channels. The total area of the oil palm plantation was 1 hectare, with an average spacing of 8–10 meters between trees. Other plantation crops surrounded the study area. The oil palm had 7 years of planting age, and the fertilizer used during initial planting was chemical fertilizer, which was later replaced with organic fertilizer.

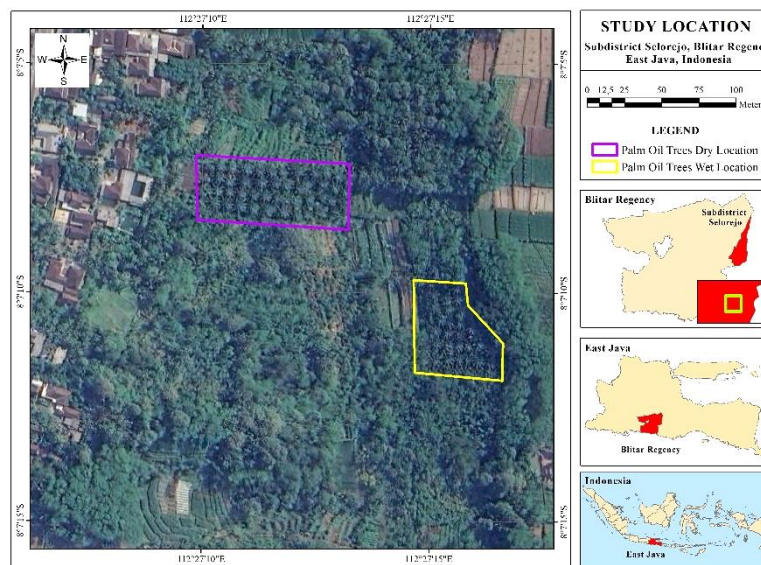


Figure 1. The location of this study was in Blitar, East Java. The yellow boxes indicate the sample area of oil palm analyzed in this study

Figure 2 shows the methodology flowchart, outlining the key steps. This study began with measuring the distance between oil palm trees using three methods: low-cost GPS, geodetic GPS, and a roll meter. The collected data were processed to determine the coordinates of each tree. Additionally, multispectral images of the oil palm trees were obtained using a MAPIR camera, which was calibrated and processed to produce Normalized Difference Vegetation Index (NDVI) data. These values were subsequently utilized to evaluate the health of the vegetation of each oil palm tree. The analysis results were amalgamated with the GPS coordinates to generate a comprehensive dataset that incorporated vegetation health data with the geographical location of each tree in the study area.

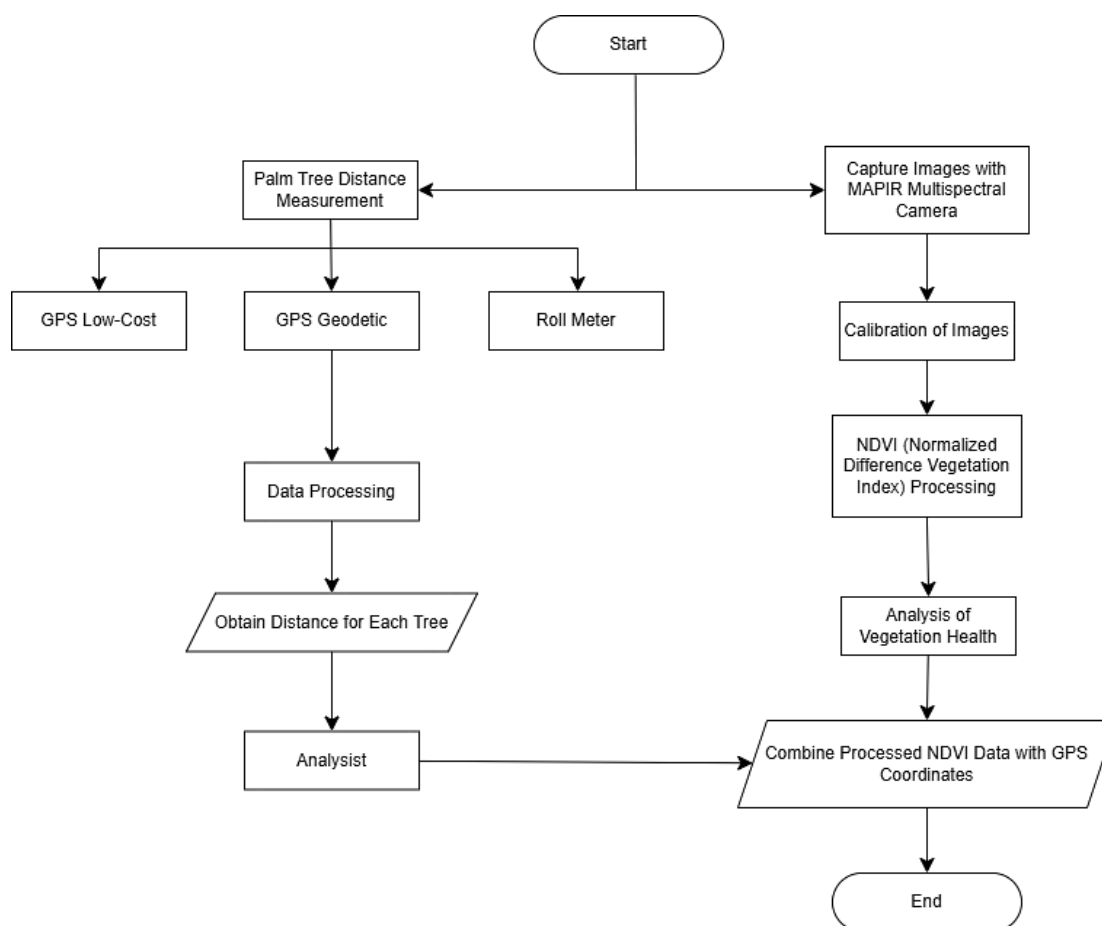


Figure 2. Study Methodology Flowchart

The methodology integrated the selection of trees based on environmental factors, the use of multispectral technology, and leaf sampling for chlorophyll analysis to identify the health of oil palm trees in the study area. Wet areas experienced frequent water flow, while dry areas received water flow only during rainfall.

2.2.1. The Oil Palm Tree Image Sampling

This research was conducted on oil palm trees in Blitar and in relation to the existence of water flow over the region. Such trees, which had access to water flow, were given the code W, while those such deprived were coded D. Leaf segmentation classified the leaves as good G and bad B. Good health-quality samples were green in color and hence possessed high levels of chlorophyll, while bad-quality ones had characteristics of yellow.

This dataset was also constructed by taking photographs of the oil palm trees with a multispectral camera with red, green, and NIR sensors. The integration of multispectral technology enhanced and broadened the approach taken towards data collection. Unlike some studies that employ UAVs for airborne imagery, this research did not make use of UAVs. Rather, the measurements were carried out by taking pictures of the trees looking up from the ground, struggling to capture individual trees. Validation of the results was carried out using a special calibration tool, MAPIR Calibration Ground Target, which was placed around the leaves such that the data obtained was able to be calibrated correctly, as shown in Figure 3. Leaf sampling was carried out using a calibration vehicle, as demonstrated by Siswantoro et al. [20] and Gantimurova et al. [21]. This calibration vehicle was positioned in front of the leaf using a special tool called the Calibration Ground Target. Figure 3 shows some pictures illustrating the methodology in use:

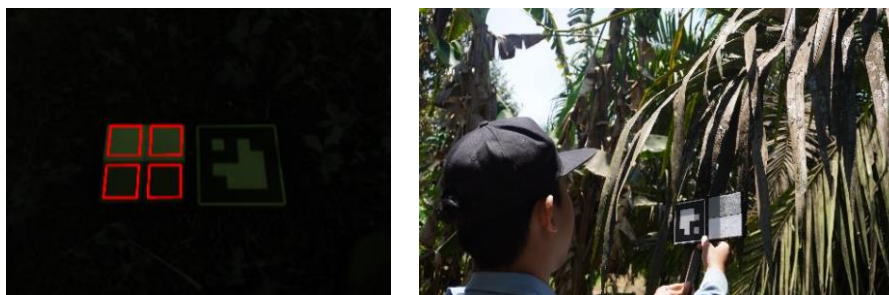


Figure 3. Application of MAPIR calibration to trees

Figure 3 shows how the MAPIR calibration approach was implemented on trees. The device was situated above the bare soil next to a dry leaf litter, and it was also interspersed with a healthy plant for purposes of data gathering. It was also used in different locations in the region of study to achieve complete calibration. The pixel values of the selected target images were contrasted to the reflectivity values of the calibration target images that are known. The pixel values were calibrated, and the survey images were taken using the MAPIR Camera Control (MCC) application. This was done in this manner so that the resultant multispectral data would be of high quality and thus suitable for analysis of plant health.

The approach in this study avoided UAV-based tree measurement and multispectral data collection techniques, which enabled it to avoid complications related to flight paths, altitude, and width adjustments. The baseball pattern, often present in UAV studies to calibrate the sensor and align it spatially, is one of the missing elements that prevented the tool from being classified in the other category. For this research, the MAPIR Survey3 RGN Multispectral Camera was used, which is a specialized stereo camera for close-sight ground-based measurements.

This helped put down the spatial control points needed to link the various images of the study area, further aiding the overall understanding of the system as demonstrated by the diagrams. This detail should facilitate further comprehension of the UAV-based multispectral camera approach regarding the measurement of trees and specific areas.

Leaf analysis is useful in diagnosing nutrient deficiencies before they become detrimental to the plant's employment. A deficiency in nutrients will cause the plant to have some symptoms like yellowing of the leaves and change of leaf color as well as reduced yield [7, 10, 22]. To determine the concentrations of chlorophyll *a* (Chl *a*) and chlorophyll *b* (Chl *b*) in the palm oil tree leaves, samples were taken from every tree that had been photographed. Chlorella content was selected for this purpose because it is one of the most important elements of the plant growth and oil palm tree health and productivity assessment. Two leaves were sampled from each photographed tree, one for each of the two conditions: good, i.e., G (good/green/healthy) health, and the other for bad yellowish, i.e., B (bad/yellowish). Leaves that were in good condition were marked G and marked B in those that were in poor condition. The examination was carried out by locating the trees and 'eyeballing' the samples for their health status.

2.2.3. Data Collection of Tree Position

Data collection of oil palm tree positions was conducted to analyze the performance of the low-cost Ublox F9R, which would be integrated into a smartphone. The coordinate results were used as positional information for each tree. The data collection analysis was performed by comparing the measurement results using GNSS Geodetic and low-cost GNSS in the Real-Time Kinematic (RTK) method with the static post-processing measurement using a GNSS Geodetic receiver [17].

The RTCM corrections from two observations using low-cost GNSS and the GNSS geodetic receiver were tied to the nearest national CORS point. Both measurements were conducted at the same point and generated consistent accuracy. RTK measurement was conducted at each oil palm tree sample, and static measurement was performed for 1 hour using the radial coordinate processing method. To obtain consistent measurement results between the geodetic receiver and low-cost GNSS, data from the same point were taken alternately. The SinoGNSS T300 geodetic GNSS provides very high accuracy, with a precision of fractions of a centimeter. On the other hand, the low-cost Ublox F9R GNSS provides quite adequate results compared to a geodetic receiver. It can be used as an effective alternative for positioning measurements that require cost efficiency without neglecting the need for relatively high accuracy [17].

2.2.4. Data Processing

In this chapter, various data processing steps are conducted, including NDVI calculation, chlorophyll analysis, and the measurement and analysis of the accuracy of oil palm tree positions. These steps are essential for understanding the condition of the vegetation and the distribution of oil palm trees based on remote sensing data. The following sub-chapters will explain each stage in detail, from the calculation of vegetation indices to the statistical tests of the accuracy of the oil palm tree position measurements.

2.2.5. NDVI Calculation

The health level of oil palm trees in this study was detected using the NDVI classification method, which was obtained by calculating the ratio between NIR and Red (R) values. NDVI is used to monitor vegetation health based on the difference between the absorption and reflectance of green leaves in the red and NIR bands of the light spectrum. The value for each pixel was estimated by dividing the difference in reflectance by the sum of NIR and red bands. NIR ranges from 0.7 to 1.1 μm , while the red band ranges from 0.58 to 0.68 μm . Usually, NDVI values range from -1 to +1, indicating healthy vegetation cover, with lower values indicating stressed vegetation and negative values suggesting open water or high-water content. The higher the NDVI values, the healthier the vegetation. The range of NDVI values during the rainy season is significantly broader compared to the dry season.

$$NDVI = \frac{NIR-RED}{NIR+RED} \quad (1)$$

where NDVI is Normalized Difference Vegetation Index, NIR is Near Infra-Red Band, and RED is Red Band.

2.2.6. Chlorophyll Calculation

To authenticate and statistically correlate, the study employed the use of a spectrophotometer to compute the chlorophyll *a* (Chl *a*) and chlorophyll *b* (Chl *b*) content and the NDVI data obtained from processing the multispectral camera. The chlorophyll-a, chlorophyll-b pigments, and total carotenoid content were evaluated principally via the method of Wellburn. It has been shown in numerous research studies that this technique is both accurate and reliable regardless of the environments, whether different solvents or spectrophotometer types were used [23]. Leaf samples from oil palm trees growing in the research location were used. Each sample was examined using three replicates for robust and reliable results. The samples were weighed and placed into 1.5 μL of microtubes, subsequently added with 1 mL of 80% acetone, and stored at 4°C for 16 hours. The solution was measured using the Genesys 10S UV-Vi spectrophotometer in several wavelengths, namely 470 nm, 646 nm, and 663 nm. The obtained absorbance was calculated using the formula [24]:

$$\text{Chl } a \left(\frac{\text{mg}}{\text{L}} \right) = 12.21A_{663} - 2.81A_{646} \quad (2)$$

$$\text{Chl } b \left(\frac{\text{mg}}{\text{L}} \right) = 20.13A_{646} - 5.03A_{663} \quad (3)$$

$$\text{Carotenoids} \left(\frac{\text{mg}}{\text{L}} \right) = (1000A_{470} - 3.27\text{Chl}_a - 104\text{Chl}_b)/198 \quad (4)$$

$$\text{Total Chlorophyll} \left(\frac{\text{mg}}{\text{L}} \right) = \text{Chl } a + \text{Chl } b \quad (5)$$

where Chl *a* is Concentration of chlorophyll *a* (mg/L), Chl *b* is Concentration of chlorophyll *b* (mg/L), Carotenoids is Concentration of carotenoids (mg/L), Total Chlorophyll is Total concentration of chlorophyll (mg/L), A_{663} is Absorbance at 663 nm, A_{646} is Absorbance at 646 nm, and A_{470} is Absorbance at 470 nm.

2.3. Analysis Method

2.3.1. Correlation Analysis

In the analysis method, the correlation between the NDVI results from the multispectral camera as well as Chl *a* and *b* content obtained from the spectrophotometer was examined [25]. The initial step was collecting NDVI data and the Chl *a* and *b* content from the same location and time, and then the correlation was calculated. Pearson correlation coefficient was the statistical method utilized, which determines the level of a linear relationship between the two variables [26, 27]. A number generated by the coefficient ranges from -1 to 1. Positive values reflect positive correlation, negative values reflect negative correlation, and zero values show no correlation at any meaningful level [28]. The results of correlation analysis will help to prove the degree of closeness that exists between NDVI and Chl *a* and *b* content [29], thus enabling the determination of representative information with respect to oil palm tree health status.

2.3.2. Accuracy of Oil Palm Tree Positions

The RTK observation method was used in conjunction with inexpensive and geodetic devices to determine the coordinate positions of oil palm trees. The study assessed the accuracy of oil palm tree positions using a range of instruments and measuring techniques, with the static approach utilizing GNSS geodetic serving as the reference value. The position measurement using other methods was evaluated for differences compared to the static-GNSS geodetic method. Data analysis was performed using the method described by Janos & Kuras [30], comparing the accuracy results of RTK measurements from geodetic receivers and low-cost devices with static measurements using the equation:

$$RD = a_{Ref} - a_{Obs} \quad (6)$$

where RD is difference between the reference and the measured coordinates, a_{Ref} is reference coordinates (static positioning), and a_{Obs} is observed coordinates (RTK positioning).

The accuracy values were analyzed against the tree canopy density, which could affect the satellite signals received by the receiver. To understand the quality of the measurement results using geodetic and low-cost receivers, a calculation of the distance from the coordinates of the observation to the reference point was carried out.

$$\Delta Horizontal = \sqrt{dx^2 + dy^2} \tag{7}$$

where $\Delta Horizontal$ is Horizontal distance of observation coordinates to reference, dx is The difference between the coordinates of the observation to the reference on the x-axis, and dy is The difference between the coordinates of the observation to the reference on the y-axis.

2.3.3. Statistic Test of Accuracy Measurement of Palm Tree Positions

The accuracy difference between low-cost and geodetic RTK observations on oil palm tree positions was assessed using a statistical test. The analysis was performed using a paired t-test commonly used when the data is not independent (paired) [31]. The common characteristic in paired cases is when one individual (study object) receives two different treatments. Despite using the same individual, two types of sample data will be obtained, namely from the first and second treatments [32].

The paired t-test was selected in this case due to the ability to compare two related or paired data sets. In the context of positioning measurement, each tree was measured twice using two different RTK methods. Considering low-cost GNSS and geodetic RTK observations originated from the same object (the same tree), the data were not independent and paired. The paired t-test is very suitable because it considers the relationship between pairs of data, thereby providing more accurate results in assessing the differences between the two measurement methods [33-35].

3. Results and Discussion

3.1. The Measurement Results of Oil palm Tree Samples with Multispectral Camera

Photographing oil palm tree samples with a multispectral camera was conducted at the study area to obtain vegetation index (NDVI) values. The results of the NDVI calculation and transformation were visualized to represent the greenness level. Figure 4 shows the visualization of NDVI results for several tree samples.

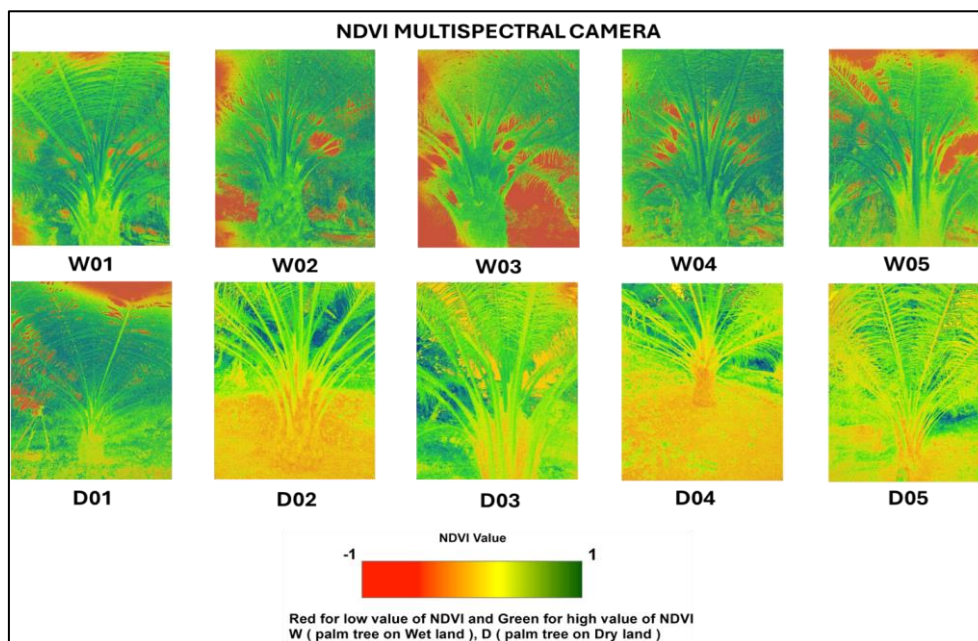


Figure 4. Several NDVI visualizations of tree samples near the water flow (W) and healthy leaf conditions (D)

Healthy leaf samples near the water flow (W-tree) tended to have high NDVI values, also characterized by bright green color throughout the tree. Tree samples with yellowish leaves far from the water flow (D-tree) tended to have relatively low NDVI, especially in the trunk. Lack of water and nutrients, as well as possible pest or disease attacks, can cause a decrease in chlorophyll content and inhibit growth.

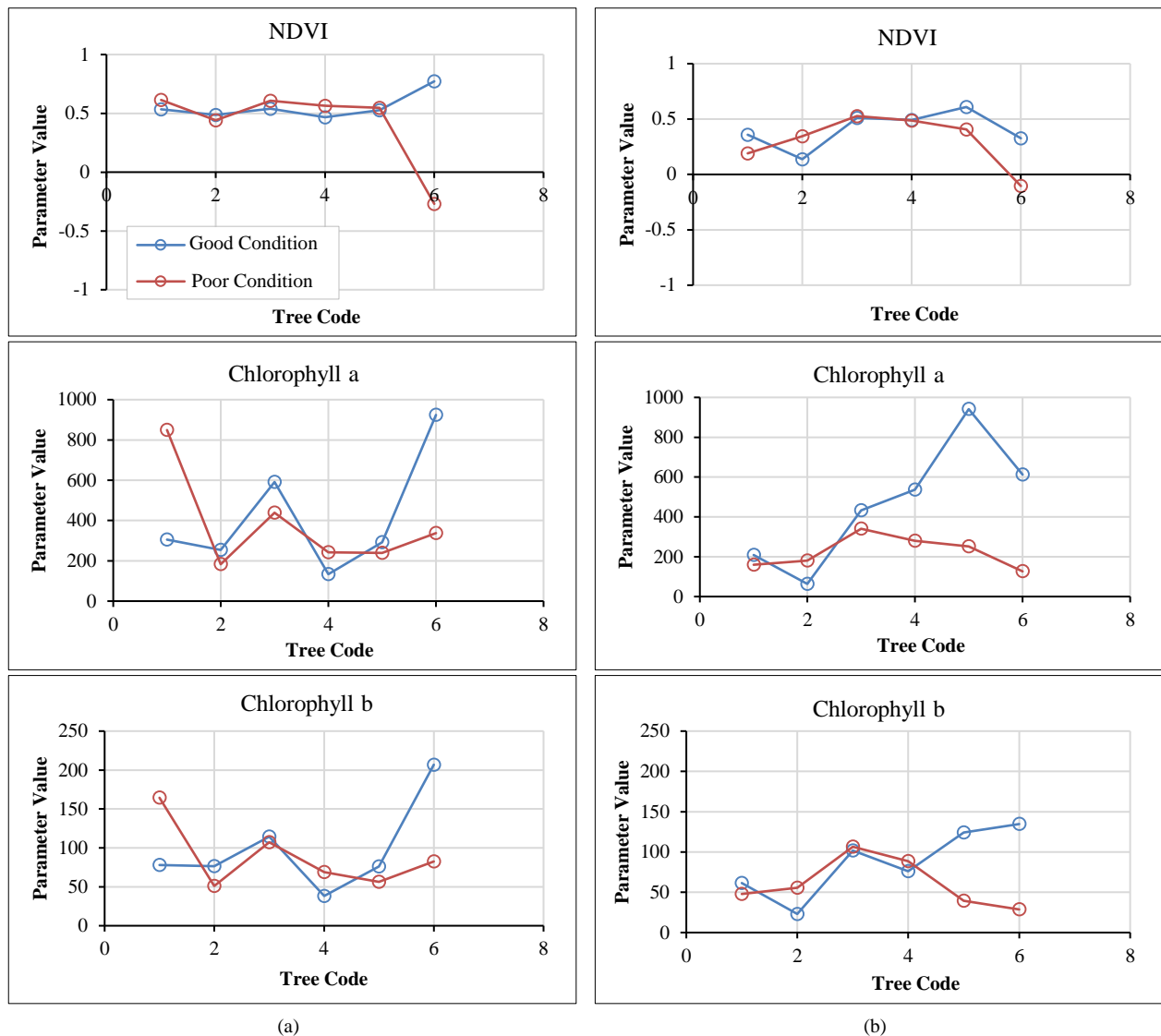


Figure 5. Comparison of NDVI, Chlorophyll a, and Chlorophyll b values (a) W-tree (b) D-tree

Based on the NDVI, Chl *a*, and Chl *b* graphs, significant differences were observed between oil palm trees located near water flow (W-tree) and those farther from water flow (D-tree), as well as between leaves in good condition (blue line) and those in poor condition (red line) (see Figure 5). NDVI values for leaves in good condition were relatively stable, ranging from 0.4 to 0.6 for the 1st to 5th trees, then dropping sharply to around -0.2 at the 6th tree and slightly increasing at the 7th tree, whereas leaves in poor condition showed greater fluctuation, ranging from 0.4 to 0.8 for the 1st to 5th trees before decreasing sharply to around -0.4 at the 6th tree.

Chl *a* value for leaves in good condition exhibited an upward trend, peaking near 1000 at the 6th tree and indicating high photosynthetic activity; in contrast, leaves in poor condition had lower and more volatile Chl *a* values, peaking around 400 at the 3rd tree. For Chl *b*, leaves in good condition followed a fluctuating trend with a peak near 200 at the 6th tree, suggesting good vegetative health, whereas leaves in poor condition were lower and more volatile, peaking around 150 at the 1st tree. Overall, oil palm trees located near water flow consistently showed higher and more stable NDVI, Chl *a*, and Chl *b* values—especially in leaves deemed to be in good condition—thereby indicating that proximity to water flow positively influences tree health and photosynthetic activity. The result is compatible with the result from the correlation of the water flow distance impact on soil fertility; when the water level decreases, the plants in the coastal area have low value NDVI [29].

3.2. Leaf Chlorophyll Content Observation Using Spectrophotometer

Data collected provided insights into the chlorophyll concentration across different samples, offering a quantitative understanding of photosynthetic efficiency. These results are crucial for evaluating the health and vigor of the plants, contributing to a deeper comprehension of physiology and growth dynamics in various environmental conditions.

The leaf samples from each oil palm tree have two conditions, namely healthy and yellowish, both having different levels of Chl *a* and Chl *b* pigments. As shown in Figure 6, the content of each pigment varied between oil palm trees. Healthy leaves showed Chl *a* content above 500 µg/g, while Yellowfish leaves had values below 300 µg/g. The Chl *b* content in healthy leaves had a concentration above 100 µg/g, while Yellowfish leaves had values below 100 µg/g.

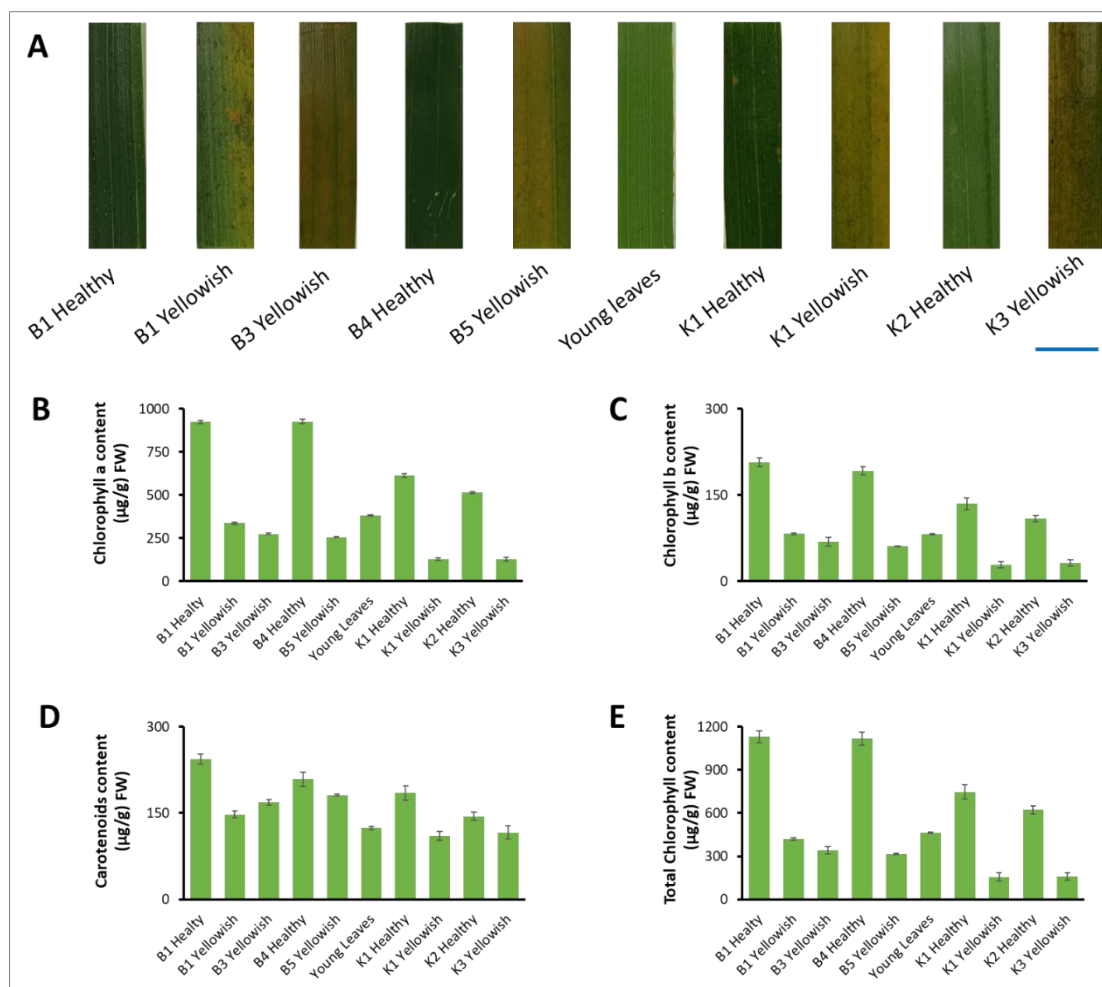


Figure 6. The measurement of pigment content. A) Various color of sample; B) The Chl a content; C) The Chl b content; D) The carotenoids content; and E) The total of Chlorophyll. The pigment value was the average from three biological replications

The colors in Figure 5a represent different shades of the leaf samples taken. These were categorized as B1 Healthy, B1 Yellowish, B3 Yellowish, B4 Healthy, B5 Yellowish, Young Leaves, K1 Yellowish, K2 Healthy, and K3 Yellowish. The samples labeled K were taken from a dry environment, while those labeled B were collected from a wet plant environment or had fairly wet soil content.

Environmental factors such as light intensity, water availability, and soil conditions affect the quality of chlorophyll in plants. Light is the main source of energy for the process of photosynthesis. Sufficient light intensity will increase photosynthesis activity, making plants produce more chlorophyll to absorb light. However, extremely high light intensity can cause damage to chlorophyll pigments and inhibit photosynthesis. The previous study showed that NDVI will slightly decrease in summertime, as it is known that the daylight is longer than night [36] with decreasing NDVI trends around 0.42 to 0.41. This causes chlorophyll degradation and decreases the levels. Water is also essential for the process of photosynthesis as it serves as a nutrient for plants. An adequate water supply is necessary for the formation and maintenance of chlorophyll. Insufficient water inhibits the process of photosynthesis and reduces chlorophyll production. In addition, drought can damage leaf structures and reduce the ability to absorb light. Soil contains various elements that affect plant growth, including nutrients, pH, and structure. Nutrients such as nitrogen, magnesium, and iron are crucial for chlorophyll synthesis. Extremely acidic or alkaline soil pH can impact nutrient availability. In general, soil with a neutral or slightly acidic pH is best for plant growth and chlorophyll production. Soil structures such as loose soil and good aeration support the efficient absorption of water and nutrients by plant roots, leading to increased chlorophyll production.

3.3. Correlation Analysis of NDVI and Chlorophyll Content of Palm Trees

The NDVI value is a calculation of the vegetation index obtained from a multispectral camera after transformation processing from the Red and NIR bands at wavelengths of 660 nm and 850 nm. The results of Chl a and Chl b were obtained from laboratory tests using a spectrophotometer on the leaf samples taken. Code G is a leaf object in good condition, and B is a leaf object in a yellowish state. The results of calculating the NDVI and chlorophyll content of each leaf sample on each tree are presented in Table 3.

Table 3. NDVI calculation results and chlorophyll content of leaf samples

Tree Code	NDVI		Chlorophyll a (µg/g)		Chlorophyll b (µg/g)	
	G	B	G	B	G	B
W01	0.5349	0.6139	305.91	849.22	77.86	164.39
W02	0.4854	0.4407	254.60	182.92	76.45	51.02
W03	0.5402	0.6069	591.29	438.85	114.57	107.04
W04	0.4672	0.5643	133.73	241.77	38.24	68.92
W05	0.5269	0.5473	291.68	239.56	76.08	56.16
W06	0.7723	-0.2698	924.14	337.07	206.82	82.44
D01	0.3582	0.1910	209.41	159.52	61.45	48.01
D02	0.1376	0.3442	63.55	180.82	23.09	55.53
D03	0.5093	0.5269	433.20	340.40	101.70	106.49
D04	0.4929	0.4854	536.64	279.69	76.07	88.66
D05	0.6088	0.4061	941.07	252.07	124.02	39.57
D06	0.3277	-0.1045	612.87	126.44	134.67	28.66
Mean	0.4801	0.3627	441.51	302.36	92.58	74.74

Based on Table 3, healthy leaf samples (G) on the W-tree had relatively high NDVI values, ranging from 0.46 - 0.77. Meanwhile, samples in the D-tree had a smaller minimum NDVI value (range 0.13 - 0.60). This is shown in Figure 7, where the average NDVI value for trees close to the water flow is higher than for those far from the water flow. This value is also directly proportional to the average chlorophyll content in the leaf samples of each tree. Leaf samples on the W-tree contain more Chl *a* and Chl *b* than those on the D-tree. In addition, leaf sample G generally had a higher chlorophyll content than B. We utilized a multiple linear regression model with NDVI G as the independent variable and chlorophyll content, represented by Chl *a* G and Chl *b* G, as the dependent variables. This approach yielded an R² value of 51%, indicating a modest improvement in the explanatory power of the model compared to the previously stated correlation. This suggests that while the relationship between NDVI G and chlorophyll content (Chl *a* G and Chl *b* G) remains moderate, the integration of a regression-based approach enhances the predictive capability of NDVI G for chlorophyll content monitoring. Future studies could explore the incorporation of additional vegetation indices or advanced modeling techniques to further strengthen this relationship.

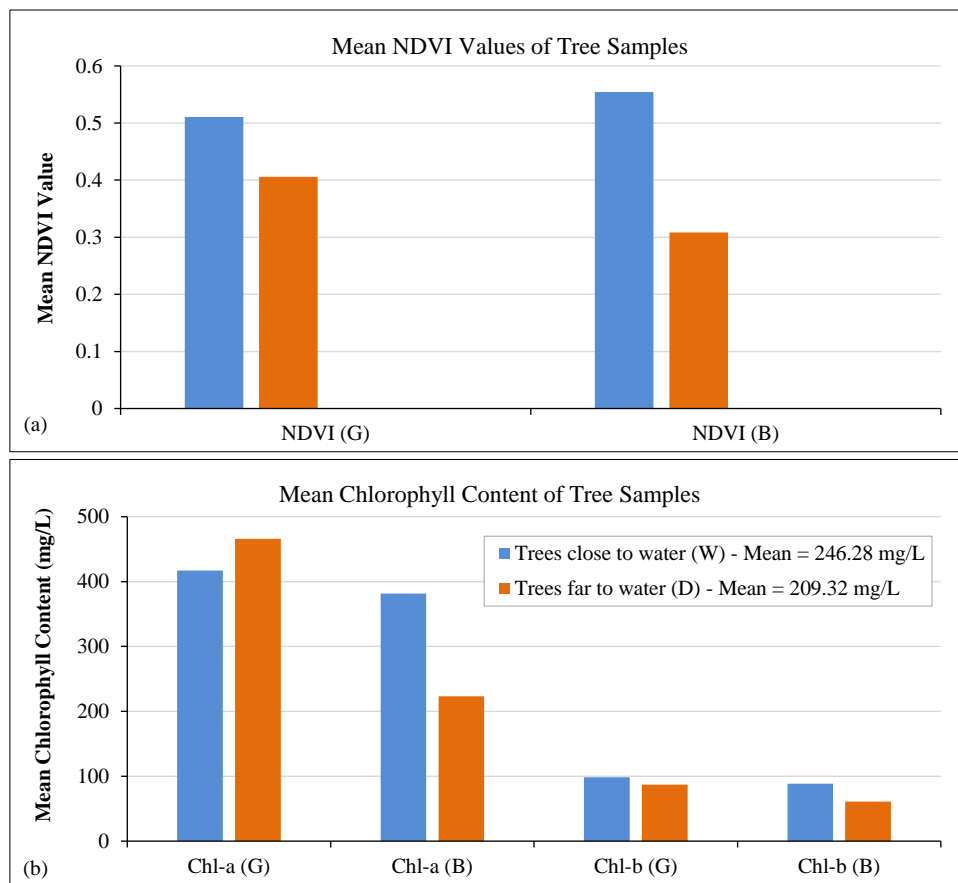


Figure 7. Graph of the average NDVI value (a) and chlorophyll content in leaf samples (b)

Additionally, leaf samples categorized as G generally displayed higher chlorophyll content than those labeled as B. This discrepancy can be attributed to the presence of soot on the surface of B leaves, which hinders photosynthesis and subsequently results in lower chlorophyll content. The soot acts as a physical barrier, reducing light penetration and impairing the leaves' ability to synthesize chlorophyll effectively. NDVI demonstrates variation in increases and decreases between symbols G and B. The average NDVI decline of -14.15% indicates that the vegetation condition in the B group tends to be more degraded compared to the G group.

Figures 8 and 9 show line fit plots and Pearson correlation results between NDVI values for Chl *a* and Chl *b*. Correlation results were calculated for each condition of the same leaf sample (healthy and yellowish), as shown in Figures 7 and 8.

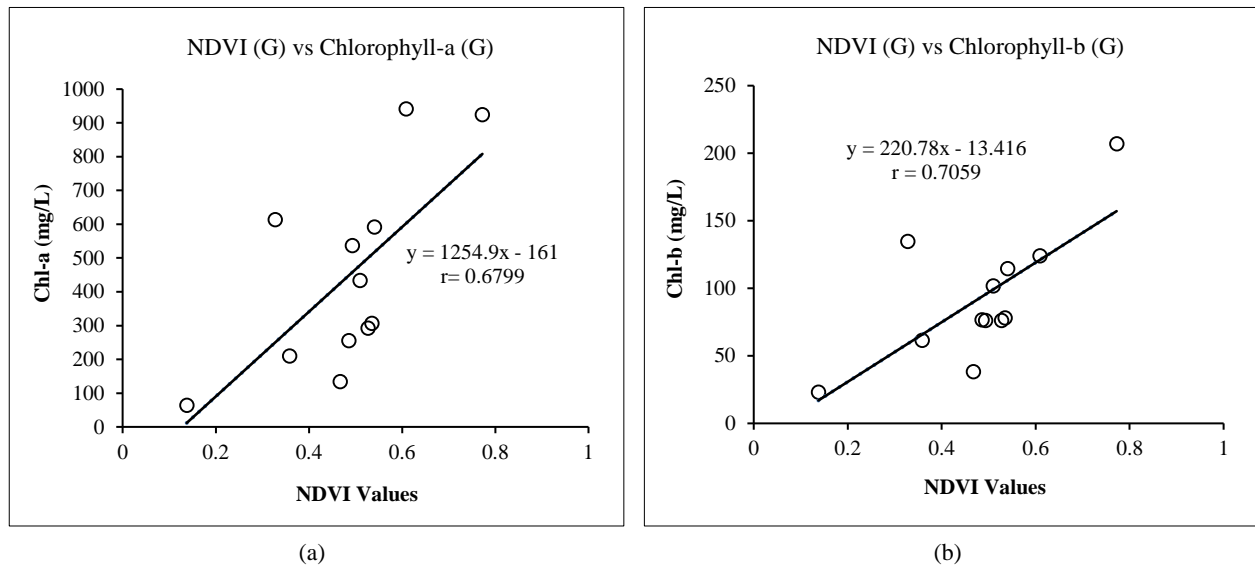


Figure 8. Correlation graph between (a) Chl *a* content and NDVI (G) and (b) Chl *b* content and NDVI (G)

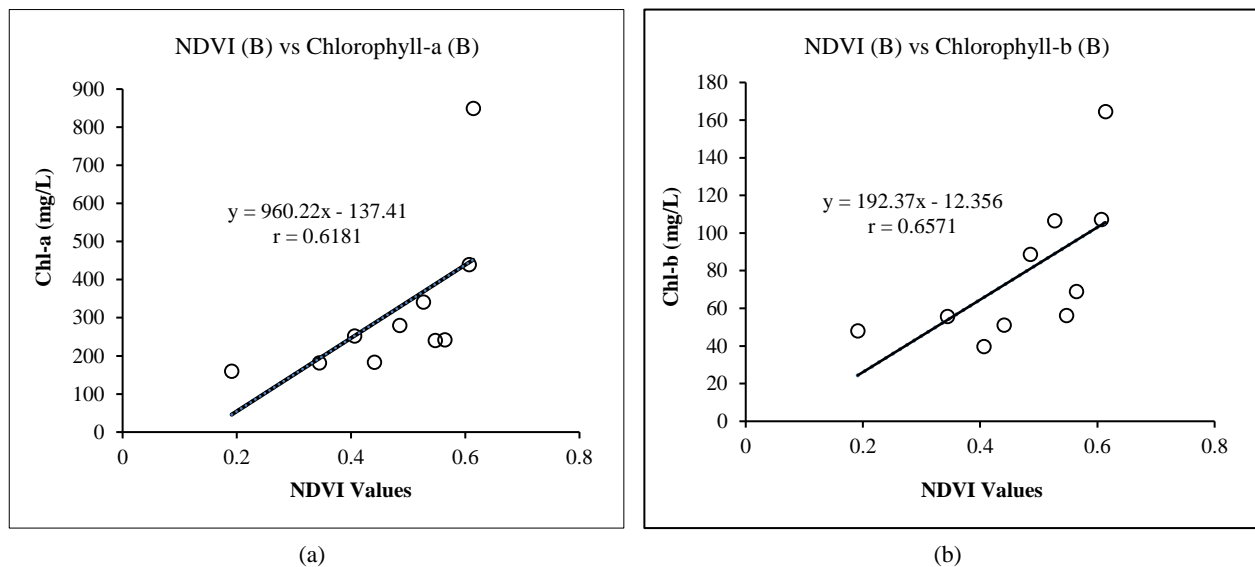


Figure 9. Correlation graph between (a) Chl *a* content and NDVI and (b) Chl *b* content and NDVI (B)

Correlation analysis aims to evaluate the relationship between the vegetation index and the chlorophyll value in plant leaves. The vegetation index value shows the greenness of the vegetation/canopy obtained from the image processing results on the MAPIR Survey3 RGN multispectral camera. The results of the correlation between the good condition plant index value (NDVI-G) and the Chl *a* value in plant leaf samples obtained a value of $r = 0.679$, where the plant vegetation index had a positive relationship with the Chl *a* value in plant leaf samples (Figure 8a). Other results also show a correlation between the good condition plant vegetation index (NDVI-G) value and the Chl *b* content value of plant leaf samples, with a value of $r = 0.705$. This suggests a positive relationship between the good condition plant vegetation index and the Chl *b* content value (Figure 8b).

The linear regression graph in Figure 7a shows the relationship between the vegetation index value and Chl *a* in plant leaves, which gives the equation $y=1254.9x-161$, and R^2 is 0.462 or 46.2%. This implies that the good condition vegetation index (NDVI-G) has a weak relationship with Chl *a* in plant leaves because the R^2 value is ≤ 0.5 . Meanwhile, the linear regression graph in Figure 7b gives the equation $y=220.78x-13.416$, and R^2 is 0.498 or 49.8%. This shows that NDVI-G has a weak relationship with Chl *b* in plant leaves. The NDVI-G correlation to Chl *b* is stronger than Chl *a*. These results are consistent with other studies. For example, Wu et al. (2008) stated that more complex vegetation indices, including TCARI/OSAVI [705,750] and MCARI/OSAVI [705,750], can provide higher correlation coefficients ($R^2 = 0.8808$ and 0.9406 , respectively) for chlorophyll estimation. This implies that integrated indices could enhance the accuracy of chlorophyll content estimation [37].

The relationship between the plant vegetation index was also analyzed on leaf samples in poor condition (NDVI-B) with chlorophyll content. These results show a correlation between the bad condition plant index value (NDVI-B) and the Chl *a* value in leaf samples, with a value of $r = 0.618$. The plant vegetation index has a positive relationship with the Chl *a* value in plant leaf samples (Figure 9a). Other results also show a correlation between the plant vegetation index in poor condition (NDVI-B) and the Chl *b* content of plant leaf samples, with a value of $r = 0.657$. This shows a positive relationship between the plant vegetation index in good condition and the value of Chl *b* content (Figure 9b). The linear regression graph in Figure 8a describes the relationship between the vegetation index value and Chl *a* content in plant leaves, which gives the equation $y=960.22x-137.41$, and R^2 is 0.382 or 38.2%. The interpretation is that the poor vegetation condition index (NDVI-B) has a weak relationship with Chl *a* in plant leaves because the R^2 value is ≤ 0.5 . The linear regression graph in Figure 8b gives the equation $y=192.37x-12.354$, and R^2 is 0.431 or 43.1% between the bad condition vegetation index (NDVI-B) value and Chl *b*. This shows that NDVI-B has a weak relationship with Chl *b* in plant leaves. However, the correlation of NDVI-B to Chl *b* is stronger than that of NDVI-B to Chl *a*.

The results indicate that the correlation between the vegetation index under good conditions (NDVI-G) and chlorophyll content is significantly stronger than under poor conditions (NDVI-B), demonstrating an improvement over previous findings [36, 38]. This study also reveals that Chl *b* content has a stronger relationship with vegetation indices in both good and poor conditions. With the value of $r = 0.705$ on Chl *b* of NDVI-G, offering a more detailed perspective compared to earlier research, which primarily focused on general correlations.

Compared to earlier studies, the findings offer enhanced insights into the role of canopy coverage and environmental factors in shaping NDVI trends by satellite image in each DOY. It shows that the chlorophyll was the most affected by the trends. The integration of these findings with previous work underscores the robustness of NDVI as a proxy for chlorophyll content and its capacity to capture variations in plant vigor under different environmental conditions; the canopy is one important factor. Based on the vine canopy volume reflected the vigor of each group of samples per DOY, which showed a good correlation between the measured canopy volume and the UAV estimated one was found in research [36]. While the previous study used both Chl *a* and Chl *b*, the recent study improved the conclusion that the most dominant type of chlorophyll in this research is Chl *b*.

The chlorophyll that indicates NDVI has also been tested on wheat. There has been a clear association between the chlorophyll content (SPAD) and NDVI with the grain yield and agronomic traits, making chlorophyll itself usable in the identification of plant N deficiency [38]. Coyne et al. [39] stated that the correlation between NDVI and Chl *b* was more significant than with Chl *a*, suggesting Chl *b* may be more sensitive to changes in the vegetation index. This implies that the evaluation of vegetation indices should consider the overall condition and emphasize the importance of detailed analysis of both chlorophyll types to obtain a more accurate picture of plant health [40].

3.4. Tree Position Data Analysis

3.4.1. Analysis of Tree Position Accuracy using the RTK Method

Determining the coordinate position of each palm tree sample was carried out using the RTK method. The objective was to examine the extent of the difference between geodetic and low-cost receiver devices for the position in forest-like obstruction conditions. The position results from the two receiver devices were validated by static differential observations using a geodetic receiver as a reference and post-processing using the radial method. Figure 10 shows the result of coordinates using the static method.

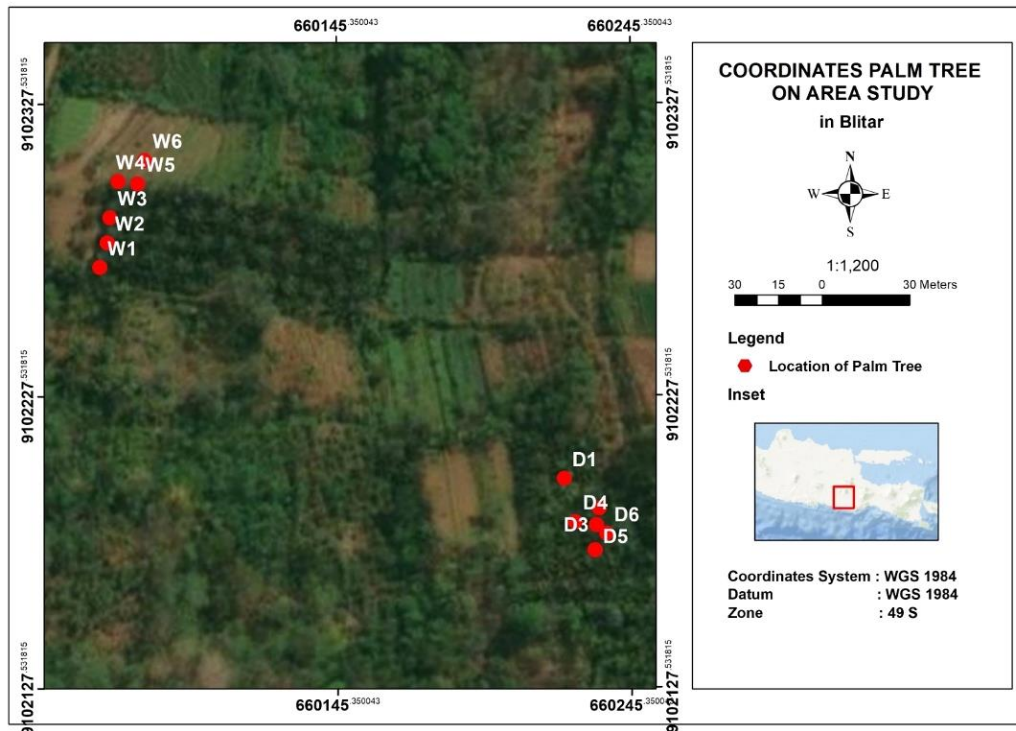


Figure 10. Coordinates of palm trees from static GNSS observations

Table 5 shows the coordinate results for 12 palm trees measured using 3 measurement methods. The differences with static-geodetic coordinates as a reference are presented in Table 4.

Table 4. Table of palm tree coordinates results using 3 measurement methods

Tree ID	Geodetic Static		Low-cost GNSS		Geodetic RTK	
	Easting (m)	Northing (m)	Easting (m)	Northing (m)	Easting (m)	Northing (m)
W1	660064.876	9102271.638	660065.036	9102271.668	660065.030	9102271.657
W2	660067.330	9102280.073	660067.483	9102279.960	660067.427	9102280.200
W3	660068.319	9102288.642	660068.314	9102288.678	660068.257	9102288.747
W4	660071.097	9102301.089	660070.940	9102301.267	660071.062	9102301.231
W5	660077.816	9102300.214	660077.857	9102300.373	660077.802	9102300.229
W6	660080.215	9102308.332	660080.095	9102308.221	660080.129	9102308.270
D1	660222.678	9102198.913	660222.745	9102198.981	660222.763	9102198.968
D2	660234.411	9102188.745	660234.555	9102188.848	660234.555	9102188.734
D3	660233.421	9102182.986	660233.579	9102183.054	660233.576	9102183.106
D4	660226.273	9102184.081	660226.445	9102184.223	660226.356	9102184.150
D5	660233.231	9102174.428	660233.402	9102174.472	660233.383	9102174.374
D6	660236.998	9102180.004	660236.898	9102180.087	660236.894	9102180.078

An analysis was conducted to compare the accuracy of observations using Geodetic RTK, Low-cost GNSS, and static observations. The differences in coordinates produced by the three methods were examined. Table 5 shows variations in coordinates in the easting and northing axes between the measurements obtained using Geodetic Static and Low-cost GNSS, as well as the differences between Geodetic Static and Geodetic RTK. These results provide insights into the variations in measurement outcomes from each method and enable a more comprehensive assessment of the accuracy and consistency of low-cost devices compared to Geodetic RTK. The low-cost GPS device relies solely on RTK NTRIP CORS BIG for corrections, which presents certain limitations compared to more advanced geodetic technologies. The accuracy differences between Geodetic RTK and Low-cost GNSS are influenced by factors such as the number of satellites, antenna quality, multipath mitigation, and resistance to cycle slip. Geodetic RTK benefits from tracking more satellites, using multi-band antennas supporting L1, L2, and L5 signals, and employing advanced algorithms to mitigate signal interference. In contrast, the Low-cost GNSS device only supports L1 and L2 signals, limiting its ability to achieve the same level of precision and making it more susceptible to errors in challenging environments.

Table 5. The difference in coordinates between Geodetic and Low-cost GNSS to static observations

Tree ID	Difference between Geodetic Static and Low-cost GNSS		Difference between Geodetic Static and Geodetic RTK	
	Easting (m)	Northing (m)	Easting (m)	Northing (m)
W1	-0.160	-0.030	-0.154	-0.019
W2	-0.153	0.113	-0.097	-0.127
W3	0.005	-0.036	0.062	-0.105
W4	0.157	-0.178	0.035	-0.142
W5	-0.041	-0.159	0.014	-0.015
W6	0.120	0.111	0.086	0.062
D1	-0.067	-0.068	-0.085	-0.055
D2	-0.144	-0.103	-0.144	0.011
D3	-0.158	-0.068	-0.155	-0.120
D4	-0.172	-0.142	-0.083	-0.069
D5	-0.171	-0.044	-0.152	0.054
D6	0.100	-0.083	0.104	-0.074
MAE	0.123	0.096	0.097	0.071
	0.155		0.120	

As shown in Table 5, the error in the low-cost GNSS coordinate results (Easting and Northing) ranges from -0.178 to 0.157, reflecting a wider variability compared to Geodetic RTK. Meanwhile, the error in Geodetic RTK has a relatively narrower range, namely -0.155 to 0.104, indicating higher precision. Geodetic RTK measurement results generally have a lower error, as indicated by the smaller Mean Absolute Error (MAE) value in the Easting and Northing directions. This demonstrates its ability to maintain consistency across measurements. Lower errors in Geodetic RTK occur in almost all tree position measurements (Figure 10), with eight absolute error values in Easting coordinates better in Geodetic RTK, three slightly better in low-cost GNSS, and the remaining showing no significant difference between the two methods. Northing coordinates, nine absolute error values were better in Geodetic RTK, while the rest were slightly better in Low-cost GNSS. These results highlight the advantages of Geodetic RTK in terms of stability and reliability, especially in challenging environments. Previous studies have also examined the accuracy of low-cost GNSS compared to geodetic RTK, showing that while low-cost coordinates can achieve comparable quality in specific conditions, they are generally less consistent under complex environmental factors [41].

The performance of Geodetic was generally better than Low-cost GNSS for measuring the position of palm trees. However, the MAE value between the two is not significantly different (0.155 m for Geodetic and 0.120 m for Low-cost). Statistical tests were carried out to evaluate whether there was a significant difference between the errors in geodetic RTK and low-cost GNSS measurements.

The larger range of differences observed in the Geodetic RTK method compared to the Static Geodetic GNSS can be attributed to environmental factors and equipment limitations. Multipath effects, caused by the reflection of GNSS signals on nearby surfaces such as leaves, tree trunks, or wet ground, are particularly significant in oil palm plantation environments. These reflections introduce delays in signal travel time, leading to inaccuracies in position measurements [6, 17]. This phenomenon is more pronounced in Geodetic RTK due to its reliance on real-time corrections, which are sensitive to such disturbances. Additionally, the hardware quality of the Geodetic RTK receivers plays a critical role. Devices with suboptimal antenna configurations struggle to mitigate multipath signals compared to Static Geodetic GNSS systems, which typically employ more robust antennas and post-processing techniques [26]. It is important to note that atmospheric factors, such as ionospheric or tropospheric disturbances, have a minimal impact in this study due to the differential correction capabilities of the RTK method [17].

To further analyse whether these differences were statistically significant, a Paired T-test was conducted, comparing the error measurements of each method on the same tree positions. The Paired T-test was used, where one individual received two different treatments (Table 6).

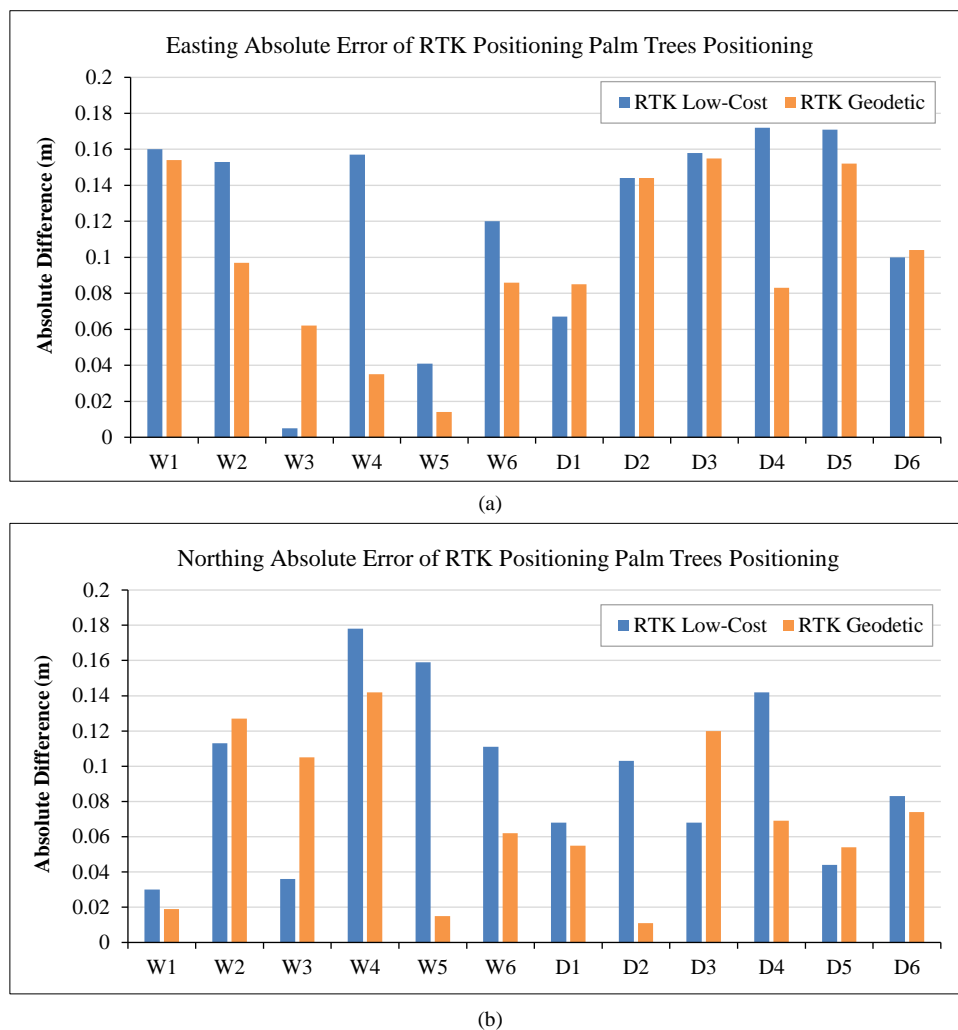


Figure 11. Absolute error graph on Low-cost GNSS (a) and Geodetic RTK (b) positioning results

Table 6. Paired Test

Null hypothesis	$H_0 : \mu_{\text{difference}} = 0$
Alternative hypothesis	$H_1 : \mu_{\text{difference}} \neq 0$
T-Value	P-Value
2.14	0.043

Based on the results of the Paired Test conducted to evaluate the differences between Geodetic and Low-cost GNSS in measuring the position of oil palm trees, a T-value of 2.14 was obtained with a P-value of 0.043. This suggests at a significance level of 5% ($\alpha = 0.05$), there is sufficient evidence to reject the null hypothesis (H_0), stating that there is no difference between the two measurement methods. However, considering the significance level used in this analysis is 2.5% ($\alpha = 0.025$), the P-Value of 0.043 indicates that the difference is not significant enough to reject the null hypothesis at the 97.5% confidence level. The difference in the measurement results between Geodetic and Low-cost GNSS cannot be considered significant at this higher confidence level.

Building on these findings, statistical analysis further validates the practicality of Low-cost GNSS systems. At a 2.5% significance level ($\alpha = 0.025$), the Paired T-test yielded a P-value of 0.043, indicating no significant difference at the 97.5% confidence level. MAE values of 0.155 m for Geodetic RTK and 0.120 m for Low-cost GNSS show minimal error differences. With a margin of error of approximately ± 10 cm, Low-cost GNSS remains a reliable and economical alternative. In the case of oil palm applications, this system is particularly suitable, as the average trunk diameter of oil palm trees exceeds 10 cm, ensuring that such small errors will not significantly impact the positioning or management of the trees. These findings highlight the cost-effectiveness and reliability of Low-cost GNSS systems, making them a practical choice for agricultural and forestry applications, where high-precision geodetic measurements are not critical.

To further optimize performance, calibration techniques such as Antenna Phase Center Calibration can improve accuracy in Low-cost GNSS systems. In oil palm plantations, where large and dense trees frequently obstruct GPS signals, GNSS reception is often poor. In such environments, where GNSS signals are frequently weak or unavailable

due to dense tree cover, IMU technology on the F9R module is essential for reliable positioning, ensuring accurate location determination when the antenna cannot optimally receive GNSS signals. Proper IMU calibration, including accelerometer and gyroscope adjustments, is crucial to ensuring accurate and stable positioning by minimizing sensor bias and drift.

3.2.4. Analysis of Distance Measurements Between Trees

Measuring the distance between trees using several GNSS measurement methods (Static Geodetic, Geodetic RTK, Low-cost GNSS) and a distometer aimed to estimate the optimal distance for planting oil palm trees. The GNSS results were validated with distometer measurements. Table 7 shows the results of GNSS measurements (Static Geodetic, Geodetic RTK, and Low-cost GNSS) and distometer.

Table 7. Comparison of distance measurements using several GNSS methods and differences with distometers

Distance	Horizontal Distance Calculation & Measurement (m)				Difference to Distometer (m)		Standard Deviation	
	Static Geodetic	Low-cost GNSS	Geodetic RTK	Distometer	Static Geodetic	Low-cost GNSS	Geodetic RTK	Low-cost GNSS
W1 - W2	8.785	8.646	8.873	8.780	-0.033	0.134	-0.093	0,093641
W2 - W3	8.626	8.758	8.587	8.670	0.044	-0.088	0.083	0,073459
W3 - W4	12.753	12.860	12.795	12.770	0.017	-0.090	-0.025	0,04695
W4 - W5	6.776	6.975	6.814	6.870	0.094	-0.105	0.056	0,086585
W5 - W6	8.465	8.161	8.371	8.390	-0.075	0.229	0.019	0,130313
D1 - D2	15.526	15.561	15.614	15.500	-0.026	-0.061	-0.114	0,049304
D2 - D3	5.843	5.876	5.713	5.790	-0.053	-0.086	0.077	0,071117
D3 - D4	7.231	7.229	7.295	7.260	0.029	0.031	-0.035	0,030934
D4 - D5	11.899	11.978	12.039	11.880	0.096	-0.098	-0.159	0,075888
D5 - D6	6.729	6.614	6.698	6.780	-0.063	0.166	0.082	0,069596
Mean Absolute Error (MAE)					0.053	0.109	0.074	

As shown in Table 7, GNSS measurements using the Static Geodetic method have a difference range of -0.075 to 0.096 meters, while Low-cost GNSS method has a difference range of -0.105 to 0.166 meters to the distometer. The Geodetic RTK GNSS measurement method has the largest difference range of -0.159 to 0.083 meters. The Geodetic RTK method was more accurate than measurements using Low-cost. Measurement using Low-cost GNSS produced less accurate results, while Static GNSS measurements had the highest accuracy indicated by the lowest MAE GNSS value of 0.053.

Low-cost GNSS measurements have a significant absolute difference, as shown in the orange graph in Figure 12. Although some measurements have results close to Geodetic RTK (W2-W3, D2-D3, and D3-D4), the performance is more accurate. Based on 10 samples of horizontal distance measurements (Figure 13), optimal planting of oil palm trees requires approximately 9.2 meters. A previous study on the position of trees explained that planting oil palm at optimal spacing requires 8-10 meters.

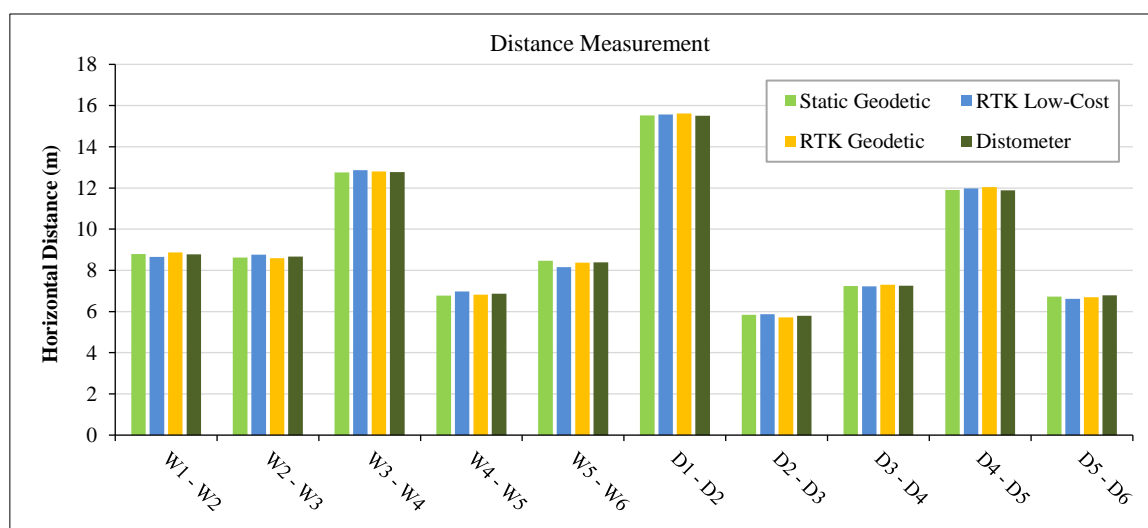


Figure 12. Graph of distance measurements between oil palm trees using several GNSS methods (Static Geodetic, Low-cost GNSS, and Geodetic RTK) and distometer

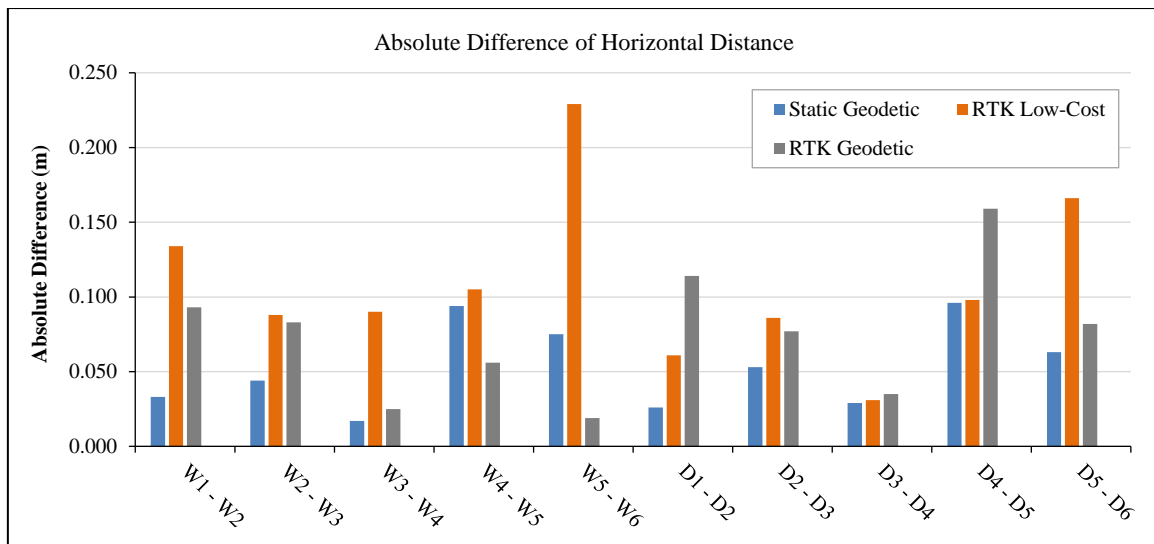
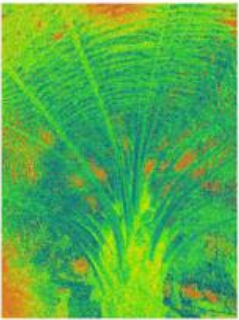
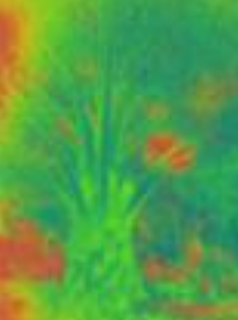
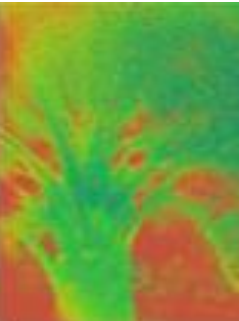
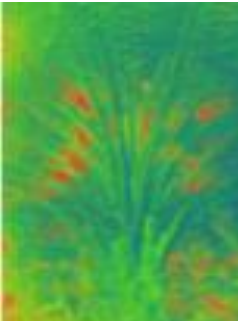


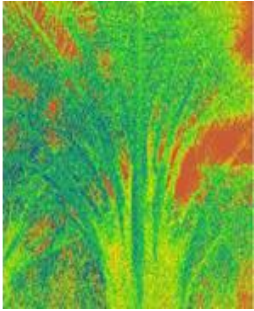
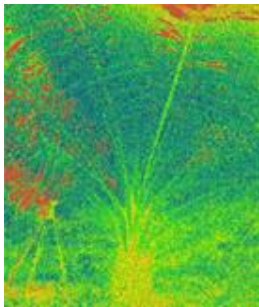
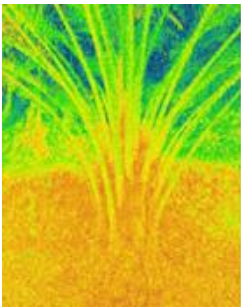
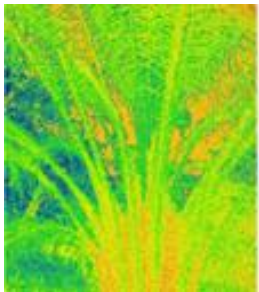
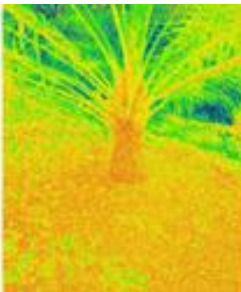
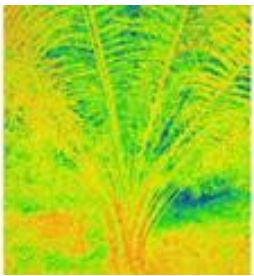
Figure 13. Graph of the absolute difference in horizontal distance measurements between oil palm trees using GNSS (Static Geodetic, Low-cost GNSS, and Geodetic RTK) to the distometer

3.5. Integration between Low-Cost GNSS and Multispectral Cameras

Determining the position of a tree using Low-cost GNSS produces a point with a global coordinate system. The integration of global tree position and the health condition of oil palm plants aims to monitor the condition in real-time by farmers using multispectral cameras. The results show the state of the oil palm plants through the spectrum from the camera with the NDVI vegetation index. This integration will produce a point position that contains information regarding the condition of oil palm plants. Table 8 shows the integration results, which can be monitored directly through a smartphone.

Table 8. Integration Result between Low-cost GNSS and Multispectral Camera

Tree	W1	Tree	W2
Easting (m)	660065.036	Easting (m)	660067.330
Northing (m)	9102271.668	Northing (m)	9102279.960
NDVI Image		NDVI Image	
Condition	Healthy	Condition	Healthy
Tree	W3	Tree	W4
Easting (m)	660068.314	Easting (m)	660070.940
Northing (m)	9102288.678	Northing (m)	9102301.267
NDVI Image		NDVI Image	
Condition	Healthy	Condition	Healthy

Tree	W5	Tree	W6
Easting (m)	660077.857	Easting (m)	660080.095
Northing (m)	9102300.373	Northing (m)	9102308.221
NDVI Image		NDVI Image	-
Condition	Healthy	Condition	UnHealthy
Tree	D1	Tree	D2
Easting (m)	660222.745	Easting (m)	660234.555
Northing (m)	9102198.981	Northing (m)	9102188.848
NDVI Image		NDVI Image	
Condition	Healthy	Condition	UnHealthy
Tree	D3	Tree	D4
Easting (m)	660233.579	Easting (m)	660226.445
Northing (m)	9102183.054	Northing (m)	9102184.223
NDVI Image		NDVI Image	
Condition	Unhealthy	Condition	Unhealthy
Tree	D5		
Easting (m)	660233.402		
Northing (m)	9102174.472		
NDVI Image			
Condition	Unhealthy		

The integration is the result of data collection points from Low-cost GPS that take points using N-TRIP mode with UTM datum coordinates according to the location zone. NDVI images from multispectral cameras can show the health conditions of oil palm plants with each tree observed from the correlation with the chlorophyll contained in the leaves.

To enhance the low-cost GNSS-based monitoring system and multispectral cameras for large-scale plantations, a well-designed system is essential to integrate multispectral cameras and GNSS into a portable device that can be carried by oil palm harvesters. The system operates automatically with a single click on a smartphone, generating one data point per click, ensuring efficiency, accuracy, and user convenience. When the harvester presses the button, the GNSS device automatically detects the tree's position, while the multispectral camera captures the tree's image. Each tree requires less than 10 seconds, and for oil palm plantations in Indonesia, with an average density of 45 trees per hectare, the estimated time required is approximately 20 minutes per hectare. Figure 14 presents the proposed system design, which integrates GNSS devices, multispectral cameras, and a smartphone-based application to ensure efficient and accurate data collection.

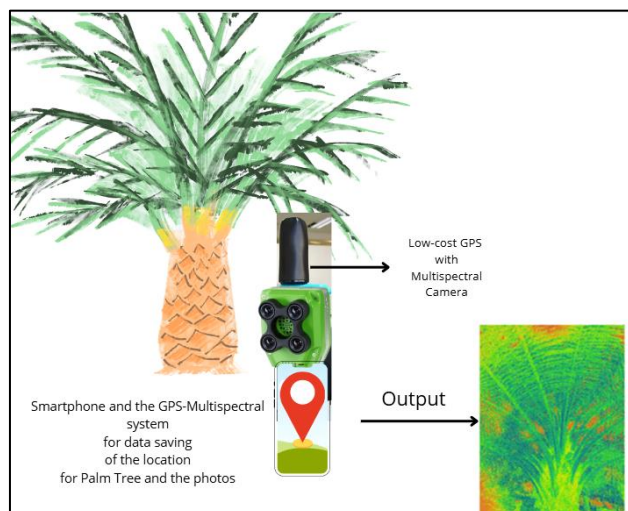


Figure 14. System design for integrating GNSS devices, multispectral cameras, and a smartphone-based application

The collected data, which includes multispectral images and GNSS coordinates, is then combined into a single file format with additional attributes such as data acquisition time and tree ID to facilitate the analysis and tracking process. Furthermore, the GNSS infrastructure must be enhanced by installing GNSS base stations at strategic locations within the plantation to improve measurement accuracy on a larger scale. Additionally, the use of low-cost GNSS devices that support N-TRIP mode with broader coverage ensures the accuracy of coordinate data.

Furthermore, GNSS infrastructure improvement is crucial, including installing GNSS base stations in strategic locations within plantation areas to enhance measurement accuracy on a larger scale. The use of low-cost GNSS devices supporting N-TRIP mode with broader coverage areas can also ensure that coordinate data remains accurate. To ensure accessibility for farmers with limited technological resources or training, a user-friendly application with a simple interface can be developed to visually display information such as color-coded maps. This should be accompanied by step-by-step guides for data interpretation and recommended actions. Basic training on using GNSS devices and interpreting multispectral data should also be provided. Additionally, training modules in the form of videos or manuals that can be accessed anytime are essential to support ease of use and understanding of this technology.

4. Conclusion

In conclusion, the findings of the study show that multispectral cameras can be employed for monitoring oil palm health. The use of NDVI as an indicator calculated from the obtained images from the multispectral camera was found to be a useful way of evaluating the oil palm trees' health by relating it to the chlorophyll of the palm leaves. Correlation analysis confirmed that the normalized difference vegetative index (NDVI-G) is valued positively with Chl *a* ($r = 0.679$) and Chl *b* ($r = 0.705$) in the plant leaves. Despite these positive correlations, the relationships were relatively weak, with the coefficient of determination (R^2) being 46.2% for Chl *a* and 49.8% for Chl *b*. This suggests that although NDVI-G is relatively stronger for Chl *b* compared to Chl *a*, it is weak for both. Of all GNSS measurement methods used, Static Geodetic was the most precise in distance measuring between the oil palm trees, with the minimum MAE being 0.053 meter and the smallest difference range -0.075 to 0.096 meter. On the contrary, although Geodetic RTK had the widest difference range from -0.159 to 0.083 meters, it performed better than the Low-cost GNSS, where the difference range was -0.105 to 0.166 meters. To enhance low-cost GNSS-based monitoring systems with multispectral cameras for large-scale plantations, a portable device for oil palm harvesters is essential. Working automatically thanks to a GNSS system, the user only needs to press their smartphone once, and the system will fetch tree locations as well as grab pictures using a multispectral camera. The process that each tree requires to complete is under ten seconds, meaning oil palm plantations would take an estimated twenty minutes per hectare. The information, together with the pictures, coordinates, and other extra definitional features requested by the user, is stored and processed for easier later analyses and geo-tracking. Moreover, base stations and low-cost GNSS devices able to work in N-TRIP mode should be installed for optimum NRTK running efficiency. Low-cost, farmer'-friendly applications and hands-on tutorials also have to be developed to assist farmers who lack adequate training or resources.

5. Declarations

5.1. Author Contributions

Conceptualization, M.N.C.; methodology, L.; software, T.B.S.; validation, M.C.L., L., and L.A.T.; formal analysis, D.K.; investigation, F.H. and T.B.S.; resources, M.N.C.; data curation, L.A.T.; writing—original draft preparation, L.A.T.; writing—review and editing, M.A.S., F.T., L., W.S.S., and D.K.; visualization, M.C.L.; supervision, M.N.C.; project administration, M.N.C. All authors have read and agreed to the published version of the manuscript.

5.2. Data Availability Statement

The data presented in this study are available on request from the corresponding author.

5.3. Funding and Acknowledgements

This research was funded by the Indonesia Collaborative Research with contract number 1661/PKS/ITS/2023. The authors are grateful to Riset Kolaborasi Indonesia 2023 for the financial support towards this study (Grant No. 1661/PKS/ITS/2023).

5.4. Conflicts of Interest

The authors declare no conflict of interest.

6. References

- [1] Dash, J. P., Pearse, G. D., & Watt, M. S. (2018). UAV multispectral imagery can complement satellite data for monitoring forest health. *Remote Sensing*, 10(8), 1216. doi:10.3390/rs10081216.
- [2] Watt, P., Meredith, A., Yang, C., & Watt, M. S. (2013). Development of regional models of *Pinus radiata* height from GIS spatial data supported with supplementary satellite imagery. *New Zealand Journal of Forestry Science*, 43(4), 1–11. doi:10.1186/1179-5395-43-11.
- [3] Marx, A., McFarlane, D., & Alzahrani, A. (2017). UAV data for multi-temporal Landsat analysis of historic reforestation: a case study in Costa Rica. *International Journal of Remote Sensing*, 38(8–10), 2331–2348. doi:10.1080/01431161.2017.1280637.
- [4] Ecke, S., Stehr, F., Frey, J., Tiede, D., Dempewolf, J., Klemmt, H. J., Endres, E., & Seifert, T. (2024). Towards operational UAV-based forest health monitoring: Species identification and crown condition assessment by means of deep learning. *Computers and Electronics in Agriculture*, 219, 108785. doi:10.1016/j.compag.2024.108785.
- [5] FAA. (2024). 2024 FAA-EASA International Aviation Safety Conference. Federal Aviation Administration (FAA), Washington, United States. Available online: https://www.faa.gov/aircraft/air_cert/international/us_eu_conference (accessed on February 2024).
- [6] Shaharum, N. S. N., Shafri, H. Z. M., Ghani, W. A. W. A. K., Samsatli, S., Al-Habshi, M. M. A., & Yusuf, B. (2020). Oil palm mapping over Peninsular Malaysia using Google Earth Engine and machine learning algorithms. *Remote Sensing Applications: Society and Environment*, 17, 100287. doi:10.1016/j.rsase.2020.100287.
- [7] Septiarini, A., Hamdani, H., Hardianti, T., Winarno, E., Suyanto, S., & Irwansyah, E. (2021). Pixel quantification and color feature extraction on leaf images for oil palm disease identification. *2021 7th International Conference on Electrical, Electronics and Information Engineering (ICEEIE)*, 1–5. doi:10.1109/iceeie52663.2021.9616645.
- [8] Mazeh, F., El Sahili, J., & Zaraket, H. (2021). Low-Cost NDVI platform for land operation: Passive and active. *IEEE Sensors Letters*, 5(10), 1–4. doi:10.1109/LSENS.2021.3112822.
- [9] Stamford, J. D., Violet-Chabrand, S., Cameron, I., & Lawson, T. (2023). Development of an accurate low cost NDVI imaging system for assessing plant health. *Plant Methods*, 19(1), 9. doi:10.1186/s13007-023-00981-8.
- [10] Marzukhi, F., Elahami, A. L., & Bohari, S. N. (2016). Detecting nutrients deficiencies of oil palm trees using remotely sensed data. *IOP Conference Series: Earth and Environmental Science*, 37(1), 12040. doi:10.1088/1755-1315/37/1/012040.
- [11] Tugi, A., Rasib, A. W., Suri, M. A., Zainon, O., Mohd Yusoff, A. R., Abdul Rahman, M. Z., Sari, N. A., & Darwin, N. (2015). Oil palm tree growth monitoring for smallholders by using unmanned aerial vehicle. *Jurnal Teknologi*, 77(26), 17–27. doi:10.11113/jt.v77.6855.
- [12] Wang, Q., Tenhunen, J., Dinh, N. Q., Reichstein, M., Vesala, T., & Keronen, P. (2004). Similarities in ground- and satellite-based NDVI time series and their relationship to physiological activity of a Scots pine forest in Finland. *Remote Sensing of Environment*, 93(1–2), 225–237. doi:10.1016/j.rse.2004.07.006.
- [13] Javid, M., Haleem, A., Khan, I. H., & Suman, R. (2023). Understanding the potential applications of Artificial Intelligence in Agriculture Sector. *Advanced Agrochem*, 2(1), 15–30. doi:10.1016/j.aac.2022.10.001.

- [14] Purwanto, E., Santoso, H., Jelsma, I., Widayati, A., Nugroho, H. Y. S. H., & van Noordwijk, M. (2020). Agroforestry as policy option for forest-zone oil palm production in indonesia. *Land*, 9(12), 1–34. doi:10.3390/land9120531.
- [15] Dhaouadi, L., Besser, H., Karbout, N., Al-Omran, A., Wassar, F., Wahba, M. S., Yaohu, K., & Hamed, Y. (2021). Irrigation water management for sustainable cultivation of date palm. *Applied Water Science*, 11(11). doi:10.1007/s13201-021-01507-0.
- [16] MAPIR Camera. (2025). Affordable remote sensing solutions for any environment. MAPIR Camera, San Diego, United States. Available online: <https://www.mapir.camera/en-gb> (accessed on February 2025).
- [17] Alkan, R. M., Erol, S., İlçi, V., & Ozulu, M. (2020). Comparative analysis of real-time kinematic and PPP techniques in dynamic environment. *Measurement: Journal of the International Measurement Confederation*, 163, 107995. doi:10.1016/j.measurement.2020.107995.
- [18] Majid, N. A., Ramli, Z., Sum, S. M., & Awang, A. H. (2021). Sustainable palm oil certification scheme frameworks and impacts: A systematic literature review. *Sustainability (Switzerland)*, 13(6), 3263. doi:10.3390/su13063263.
- [19] Absalome, M. A., Massara, C. C., Alexandre, A. A., Gervais, K., Chantal, G. G. A., Ferdinand, D., Rhedoor, A. J., Coulibaly, I., George, T. G., Brigitte, T., Marion, M., & Jean-Paul, C. (2020). Biochemical properties, nutritional values, health benefits and sustainability of palm oil. *Biochimie*, 178, 81–95. doi:10.1016/j.biochi.2020.09.019.
- [20] Siswanto, J., Artadana, I. B. M., & Siswanto, M. Z. F. N. (2022). Leaf geometric properties measurement using computer vision system based on camera parameters. *International Conference on Informatics, Technology, and Engineering 2021 (InCITE 2021): Leveraging Smart Engineering*, 2470, 050008. doi:10.1063/5.0080190.
- [21] Gantimurova, S., Parshin, A., & Erofeev, V. (2021). GIS-based landslide susceptibility mapping of the circum-baikal railway in Russia using UAV data. *Remote Sensing*, 13(18), 3629. doi:10.3390/rs13183629.
- [22] Sabri, S. A., Mohd., Endut, R., B. M. Rashidi, C., R. Laili, A., A. Aljunid, S., & Ali, N. (2019). Analysis of Near-infrared (NIR) spectroscopy for chlorophyll prediction in oil palm leaves. *Bulletin of Electrical Engineering and Informatics*, 8(2), 506–513. doi:10.11591/eei.v8i2.1412.
- [23] Saini, A., Singh, J., & Kant, R. (2022). Comparative Study of Estimation Methods for Efficient Extraction of Chlorophyll a and Carotenoids Using Different Solvents. *Bulletin of Pure & Applied Sciences- Botany*, 41b(2), 79–86. doi:10.5958/2320-3196.2022.00009.x.
- [24] Ali, K. A., Noraldeem, S. S., & Yaseen, A. A. (2021). An Evaluation Study for Chlorophyll Estimation Techniques. *Sarhad Journal of Agriculture*, 37(4), 1458–1465. doi:10.17582/journal.sja/2021/37.4.1458.1465.
- [25] Khorramnia, K., Khot, L. R., Shariff, A. R. B. M., Ehsani, R., Mansor, S. B., & Rahim, A. B. A. (2014). Oil palm leaf nutrient estimation by optical sensing techniques. *Transactions of the ASABE*, 57(4), 1267-1277. doi:10.13031/trans.57.10142.
- [26] Gamon, J. A., Field, C. B., Goulden, M. L., Griffin, K. L., Hartley, A. E., Joel, G., Penuelas, J., & Valentini, R. (1995). Relationships between NDVI, canopy structure, and photosynthesis in three Californian vegetation types. *Ecological Applications*, 5(1), 28–41. doi:10.2307/1942049.
- [27] Silva, S. A. S., Ferraz, G. A. S., Figueiredo, V. C., Volpato, M. M. L., Machado, M. L., Silva, V. A., ... & Bambi, G. (2024). Spatial variability of chlorophyll and NDVI obtained by different sensors in an experimental coffee field. *Agronomy Research*, 22(X), 1-16. doi:10.15159/AR.24.037.
- [28] Šverko, Z., Vrankić, M., Vlahinić, S., & Rogelj, P. (2022). Complex Pearson Correlation Coefficient for EEG Connectivity Analysis. *Sensors*, 22(4), 1477. doi:10.3390/s22041477.
- [29] Rodríguez-López, L., Duran-Llacer, I., González-Rodríguez, L., Abarca-del-Rio, R., Cárdenas, R., Parra, O., Martínez-Retureta, R., & Urrutia, R. (2020). Spectral analysis using LANDSAT images to monitor the chlorophyll-a concentration in Lake Laja in Chile. *Ecological Informatics*, 60, 101183. doi:10.1016/j.ecoinf.2020.101183.
- [30] Janos, D., & Kuras, P. (2021). Evaluation of Low-Cost GNSS Receiver under Demanding Conditions in RTK Network Mode. *Sensors*, 21(16), 5552. doi:10.3390/s21165552.
- [31] Rosner, B. (1982). A Generalization of the Paired t-Test. *Applied Statistics*, 31(1), 9. doi:10.2307/2347069.
- [32] Elaksher, A., Ali, T., Kamtchang, F., Wegmann, C., & Guerrero, A. (2020). Performance analysis of multi-GNSS static and RTK techniques in estimating height differences. *International Journal of Digital Earth*, 13(5), 586-601. doi:10.1080/17538947.2018.1550118.
- [33] Abid, M. A., Husein, H. N., & Hamed, N. H. (2020). Analysis of Error in Geodetic Networks using Different Observation Methods. *IOP Conference Series: Materials Science and Engineering* 737(1), 012234. doi:10.1088/1757-899X/737/1/012234.
- [34] Štern, A., & Kos, A. (2018). Positioning performance assessment of geodetic, automotive, and smartphone GNSS receivers in standardized road scenarios. *IEEE access*, 6, 41410-41428. doi:10.1109/ACCESS.2018.2856521.

- [35] Paziewski, J., Sieradzki, R., & Baryla, R. (2018). Multi-GNSS high-rate RTK, PPP and novel direct phase observation processing method: Application to precise dynamic displacement detection. *Measurement Science and technology*, 29(3), 035002. doi:10.1088/1361-6501/aa9ec2.
- [36] Caruso, G., Tozzini, L., Rallo, G., Primicerio, J., Moriondo, M., Palai, G., & Gucci, R. (2017). Estimating biophysical and geometrical parameters of grapevine canopies ('Sangiovese') by an unmanned aerial vehicle (UAV) and VIS-NIR cameras. *VITIS-Journal of Grapevine Research*, 56(2), 63–70. doi:10.5073/vitis.2017.56.63-70.
- [37] Zeng, Y., Hao, D., Huete, A., Dechant, B., Berry, J., Chen, J. M., ... & Chen, M. (2022). Optical vegetation indices for monitoring terrestrial ecosystems globally. *Nature Reviews Earth & Environment*, 3(7), 477-493. doi:10.1038/s43017-022-00298-5.
- [38] Kizilgeci, F., Yildirim, M., Islam, M. S., Ratnasekera, D., Iqbal, M. A., & Sabagh, A. E. L. (2021). Normalized difference vegetation index and chlorophyll content for precision nitrogen management in durum wheat cultivars under semi-arid conditions. *Sustainability (Switzerland)*, 13(7), 3725. doi:10.3390/su13073725.
- [39] Coyne, P. I., Aiken, R. M., Maas, S. J., & Lamm, F. R. (2009). Evaluating yield tracker forecasts for maize in Western Kansas. *Agronomy Journal*, 101(3), 671–680. doi:10.2134/agronj2008.0146.
- [40] Jopia, A., Zambrano, F., Pérez-Martínez, W., Vidal-Páez, P., Molina, J., & Mardones, F. de la H. (2020). Time-series of vegetation indices (VNIR/SWIR) derived from sentinel-2 (A/B) to assess turgor pressure in Kiwifruit. *ISPRS International Journal of Geo-Information*, 9(11), 641. doi:10.3390/ijgi9110641.
- [41] Taufik, M., Yuwono, Cahyadi, M. N., & Putra, J. R. (2019). Analysis level of accuracy GNSS observation processing using u-blox as low-cost GPS and geodetic GPS (case study: M8T). *IOP Conference Series: Earth and Environmental Science*, 389, 012041. doi:10.1088/1755-1315/389/1/012041.